100 GHz Multiple Colliding Pulse Generation from Cleaved Facet-free Multi-section Semiconductor Laser Diode

Robinson C. Guzmán Martínez[1], Jessica César Cuello[1], Alberto Zarzuelo[1], Mu Chieh Lo[2], Muhsin Ali[1], Guillermo Carpintero del Barrio[1]
[1] University Carlos III of Madrid, UC3M, Electronics Technology Department, [2] University College London, Department of Electronics and Electrical Engineering
e-mail: rcguzman@ing.uc3m.es

***Abstract*—We present a monolithically integrated mode-locked laser (MLL) with 25 GHz fundamental repetition rate frequency, which has been designed to operate in a fourth-order colliding regime, to generate 100 GHz. This device has been fabricated within a multi-project wafer (MPW) run in an InP-based active-passive generic foundry. The Fabry-Perot laser resonator, of around 1.66 mm length, is defined by two on-chip reflectors, eliminating the need of cleaved facet. Three saturable absorber sections are symmetrically located by spacing them a quarter of this total length, dividing the cavity into four gain segments. We show that this structure can generate an electrical beat note at 25 GHz as well as 100 GHz, with a linewidth of 350 kHz and 150 kHz, respectively, operating in passive operation regime.**

***Index Terms*—Semiconductor laser, saturable absorber, multimode interference reflectors, electrical linewidth, multiple colliding pulses, mode-locked laser.**

I. Introduction

PASSIVE mode-locked (PML) laser structures capable of being integrated into Photonic Integrated Circuits (PIC) are an alternative to achieve on-chip sources of multiples phase-locked optical wavelengths. These lasers, achieving Repetition Rates (RR) in microwave (MW, 300 MHz - 300 GHz) and Terahertz (THz, 0.1 - 10 THz) frequency ranges have been considered promising device in microwave photonics [1], communications [2], optical division multiple-access systems [3] and frequency comb generator [4], [5]. The structure requires a Fabry-Perot (FP) cavity with gain and saturable absorber (SA) sections, which depending on the arrangement can generate different RR frequencies. The advantage of our monolithic integrated approach is its chip-scaled compactness, which allows them to be placed within a PIC with additional functionality on a single chip, and simplicity of DC operation. The advantage of the passive mode-locking operation regime is that it requires only constant current and voltage sources for the device to generate the pulsed signal. However, the generated signal usually lacks the required stability and is not synchronized to any other signal. In order to improve these limitations, hybrid mode-locking operation regimes are used, in which superimposed to reverse voltage, we apply a continuous wave (CW) signal with a frequency equal to the repetition rate. The stability of the RR is now determined by the CW signal source. Recently, using a different technology platform a Si-based 20 GHz QD-MLL with a wide span [6] of the optical comb has been used to transmit several terabits of data in a different wavelength window. Furthermore, there are other optical techniques which can generate a very wide optical frequency comb with high RR (>100 GHz) e.g. SiN based ring resonator [7] using a simple diode laser, these type of devices use two different technologies for the fabrication of each component making the overall optical integration more complex. When high RRs (>100 GHz) are desired, the most straightforward solution is to decrease the resonator length of the MLL to few hundreds of μm (<400 μm). however, there is a limit to the smallest gain section that will produce sufficient optical gain to overcome the resonator loss. For this reason, harmonic mode-locked (HML) structures have been investigated to overcome this limit and increase the RR without reducing the cavity length, by generating different pulses per round trip, effectively multiplying the fundamental RR of the cavity [8]. Harmonic mode-locking has been demonstrated using a variety of techniques, from colliding pulse mode-locked lasers (CPMLLs) [9],[10], coupled-cavity mode-locking [11], methods based on the wavelength selectivity of distributed Bragg reflector (DBR) grating [12] or compound cavity laser [13]. In the CPMLL structure, one saturable absorber is located at the laser resonator center, which results in two optical-counter-propagating pulses in the cavity that meet at the SA. Therefore, the RR frequency is now twice the fundamental round trip frequency.

Manuscript received June 21, 2019. This work was supported in part by the European Union's Horizon 2020 (Marie Skłodowska-Curie grant agreement No. 713694 FiWiN5G), and the Spanish Ministerio de Economia y Competitividad thourgh Programa Estatal de Investigación, Desarrollo e Inovación Orientada a los Retos de la Sociedad thougth grant iTWIT, TEC2016-76997-C3-3-R.

R. C. Guzman, J. César, A. Zarzuelo, M. C. Lo, M. Ali and G. Carpintero are with the Department of Electronics Technology, University Carlos III de Madrid, Leganés 28912, Spain (e-mail: rcguzman@ing.uc3m.es).

A. Zarzuelo is collaborating in SENER aerospace.

M. C. Lo is with the Department of Electronics and Electrical Engineering, University College London, Torrington Place, London, WC1E 7JE

Evolving from the CPMLL structure, the multiple colliding pulse mode-locking lasers (MCPMLL) features multiple SAs between gain sections, allowing to increase the RRs multiplication factor above 2, has been extensively investigated [14]-[17]. In this technique, the SAs are placed at defined fractional positions of the cavity length in order to generate the N^{th} order harmonic signal. It is worth noticing that these structures [6]- [9], [11]–[16] use the cleaved facet of the chip as a mirror or reflector. In order to avoid using the cleaved facet for the laser mirrors, we have used on-chip multimode interference (MIR) reflectors [18]. Several works have demonstrated the wide applicability of such mirrors [19], [20], which are simple to create in lithography and have greater fabrication tolerances than grating mirrors. On-chip mirrors are key to take full advantage of the integrated potential, enabling to further process the optical signal on the PIC [21]. We have recently reported 100 GHz MIR-based MCPMLL [22] used to generate millimeter (MMW) carries for wireless data transmission [23].

In this work, we report the fabrication and experimental investigation of a multi-section MCPMLL diode structure employing three SAs and four semiconductor optical amplifiers (SOAs) based gain sections. The structure has been designed for the 100 GHz millimeter-wave carrier generation multiplying the 25 GHz the fundamental RR of the cavity as in [21]. The difference of this structure with respect to that in [21] is that this one is symmetric, having additional SA and gain section within the FP cavity, enhancing the performance of the structure. The frequency achieved with the device lies into the F-Band (90 – 140 GHz) of the millimeter-wave spectrum. This work is focused on demonstrating the stability of the electrical beating in hybrid mode-locking operation regimen using a subharmonic RF signal (25GHz and 50 GHz) injected into the SAs. The Photonic Integrated Circuit (PIC) presented in this work was designed and fabricated by the Smart Photonics platform using a generic passive-active integration technology. The chip is fabricated in a Multi-Project Wafer (MPW) project [24]. We have designed our MCPMLL combining different building blocks of their platform.

II. Device Description

As we pointed out previously, the main characteristic of the MCPMLL cavity structure that we present is the resonator symmetry with respect to the central SA, as shown in Fig. 1. Fig. 1 shows a schematic of the structure layout. The FP laser cavity is defined by the MIR mirrors at both extremes. The MIR derive from the standard multimode interference coupler (MMI), allowing for an accurately defining of the total length of the FP cavity. Within this cavity, four gain sections can be observed, in between which three equal SA sections are introduced. Both SOAs and SAs sections use the same active layer stack during the fabrication based on InGaAsP/InP quantum well gain media. The SAs are created by reverse biasing with voltage a small SOA. In order to reduce the number of contacts in the experiment, the gain sections are connected by pairs. The contacts of the two 180 µm long outer SOAs are shorted together. In the same way, the two 350 µm long inner SOAs are also shorted together. This allows us to reduce the number of contacts required in the experiment while allowing to inject different current levels into the short and long SOAs to balance the optical pulse powers collinging in the 20 µm long SAs. In order to reduce contacts, while maintaining symmetry in the device, the contacts for the two SA sections at the extremes have been shorted. Electrical isolation sections of 20 µm long are placed between every two adjacent active sections in order to avoid undesirable back current flows and device malfunction. For the purpose of achieving the fourth harmonic multiple colliding regimes, the position of the three SAs ought to be very accurate. These are spaced by one-quarter of the total cavity length (L/4), around 420 µm long. The passive waveguides are deeply etched, with minimum bending radius of 100 µm. These MIRs structures are deeply etched 45o mirrors which can be placed at suitable locations reflecting back the light by the total internal reflection of the component [10]. The length of each MIR is around 55 µm long, with a reflectivity of 60% and 40% for the ports 1 and 2, respectively. The MCPMLL has two available optical outputs named OutP0_0 and OutP0_1. The output OutP0_0 provides the pulses from the leftmost MIR of the MCPMLL, while output OutP0_1 includes a 400 µm long Boost SOA to boost the optical power at the output from the rightmost MIR, after going through a 2x2 MMI. This 2x2 MMI is inserted to split in two the optical signal from rightmost MIR. As we have already described, one forms the output at the edge of the chip after a boost SOA, while the other 2x2MMI output is used within an on-chip optical signal processing function that is not relevant for the present case. The on-chip MIRs contribute to the total cavity length (L) which is around 1.66 mm, corresponding to a cavity fundamental round-trip frequency of 25 GHz. The MCPMLL design occupies an area of 1.66 x 0.77 mm2 without taking into account the optical components on the right-hand side of the structure. To minimized and avoid parasitic back-reflections, the two optical output waveguides corresponding to OutP0_0 and OutP0_1, are tilted upwards by 7º, as shown in Fig. 1. The cleaved facet of the chip is anti-reflection coated (AC) decreasing the power reflection coefficient to <10-4.

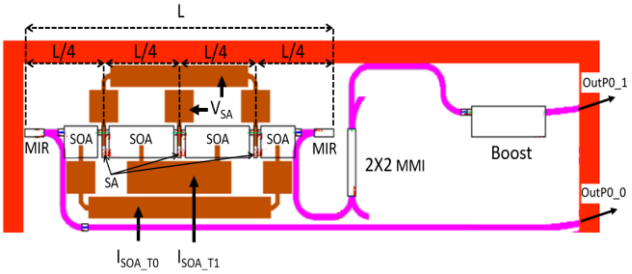

Fig. 1. Schematic of the layout of the MCPMLL. The structure is made of four gain sections and three SA sections. Symmetrically placed around the central SA

III. Characterization Setup Description

For the characterization of the MCPMLL, firstly, the chip is glued with a thermal conductive paste and mounted on a submount. The electrical contact pads for the outer, the inner SOAs and the metal layer of the boost, are wire-bonded to individual DC tracks on the submount. The two outer SAs which are short-circuited and connected by a pad extension and, along with the pad extension of the SA located at the midpoint of the FP cavity, are wire-bonded to the same RF track on the submount allowing for the system to work in both passive operation and hybrid operation regimes. In this work, all SAs are driven by the same DC and RF signal. The submount is mounted on a temperature-controlled cooper chuck and the chip is temperature stabilized at 16 ºC by a thermos-electric cooler (TEC). The characterization of the MCPMLL is carried out by using the setup depicted in Fig. 2(a). The two pairs of SOAs and the boost are forward-biased through direct probing on each DC track on the submount with DC probe needles. Each DC probe needle is connected to an independent current source -Thorlabs PRO8000 laser diode driver-. The SAs are reverse-biased through a 40 GHz RF Ground-Signal-Ground (GSG) probe. The RF probe is connected to an external bias tee with an electrical bandwidth up to 67 GHz. This bias tee helps us to inject both the DC and the RF signals into the SAs at the same time achieving passive or hybrid operation regime. Agilent E3631A voltage source supplies the reverse-bias voltage to drive the SAs. An anti-reflection coated lensed fiber (ACLF) to collect the outgoing light from one of the two output waveguides of the laser is used. In fact, an optical circulator spliced to the ACLF to prevent any back-light reflection to the chip from any optical component connected after it is used. As sketched in Fig. 2(a), a chain of optical splitters (OS) are connected in a series way in order to connect the different measurement equipments used for the characterization of the chip. First, the 1% output port of the 99:1 OS is used to connect an Optical Power Meter (OPM) to constantly monitor the optical power of the laser while the other 99% output port is connected to a 90:10 OS. Next, an Optical Spectrum Analyzer (OSA) is connected to the 10% output port for the measurement and recording of the optical signal whilst the 90% branch is followed by another OS used to split in two the optical signal with a 50:50 ratio. The reason for splitting the optical signal is that the R&S FSW-50 Electrical Spectrum Analyzer (ESA) used for the measurement and recording of the generated electrical signal has a full bandwidth of up to 50.1 GHz. However, this ESA has the option of measuring electrical signals above its maximum frequency using an external mixer head with the required frequency band. The MCPMLL generates an optical spectrum with frequency spacing of 25, 50 and 100 GHz. Therefore, a W-band (75 – 110 GHz) mixer head to downconvert high-frequency signals is used. Two optoelectronic (OE) converters to turn the optical signal into an electrical signal are used. These OE converters are type PIN-photodiode and have different -3 dB bandwidths for each frequency range.

IV. Measurement Results

In this work, firstly, the optical power is measured at the output port OutP0_0. The boost located at the other output port is kept open, i.e. without DC current injection. The measurement of light vs current (LI) characteristic curves of the laser is presented in Fig. 2. The current injected into the outer SOAs (I_{SOA_T0}) is set to 10 mA (Fig. 2(b)), 20 mA (Fig. 2(c)) and 30 mA (Fig. 2(d)) while the current injected into the inner SOAs (I_{SOA_T1}) is swept from 0 to 100 mA in 2 mA steps and, at the same time V_{SA} is set to different reverse-bias voltage from 0 to 2 V in 0.5 V steps. As shown in Fig. 2(b), for I_{SOA_T0} = 10 mA, the laser has a threshold current level from 35 to 50 mA as the SAs reverse-bias voltage goes from 0 V to 2V. The highest fiber-coupled power exceeds 0.15 mW for V_{SA} = 0 V, however, as V_{SA} reverse-bias voltage is greater than 0 V, the output power drops almost a third of the maximum optical power. The optical output power decreases up to ~0.04 mW as V_{SA} is set to -2V. When I_{SOA_T0} is greater than 10 mA, as shown in Fig. 2(c) and Fig. 2(d), the threshold current level decreases with respect to the first case for both cases as V_{SA} goes down from 0 to -2V. For I_{SOA_T0} = 20 mA the threshold current level goes from 25 to 28 mA, as for I_{SOA_T0} = 30 mA the threshold current level goes from 22 to 25 mA. In the same manner, the output optical power delivered by the device under both different biasing conditions increase, but decreasing for SAs reverse-bias voltage of 0 V down to -2 V. Next, in order to know the influence of the boost on the output optical power at the output port OutP0_1 when a DC current signal is injected into its gain section, the LI characteristic curve of the boost is measured. The biasing conditions of the rest of the optical components involved in the MCPMLL structure are kept off, i.e. both the current sources and the voltage source their output are set off. As we can see in Fig. 3(a), the current injected into the gain section is swept from 0 to 120 mA in 2 mA steps getting a threshold current level about 4 mA increasing the optical power as the injected DC current increases. However, the maximum optical power generated by the boost is achieved when the saturation condition is reached (I_{Boost} ~ 88 mA). By going further the saturation condition the optical power decreases thus, for the safety of the boost, the maximum DC current injected should be less than 88 mA. Secondly, in order to find out what is the minimum DC current value injected into the boost to overcome the losses introduced by the 2x2 MMI an LI curve is done. The LI curve is depicted in Fig. 3(b) for I_{SOA_T0} = 10 mA, I_{SOA_T1} from 0 to 100 mA, V_{SA} = 0 V and I_{Boost} at 10 mA, 20 mA and 30 mA. As we can see in Fig. 3(b) the maximum optical power delivered by the device is ~160 µW (red solid line) at the output port OutP0_0. Injecting 10 and 20 mA into the boost the optical powers reached for both cases with respect to the red solid line are ~4.2 dB and ~0.8 dB Therefore, to overcome the losses introduced by the 2x2 MMI, the I_{Boost} DC current injection must be greater than 20 mA.

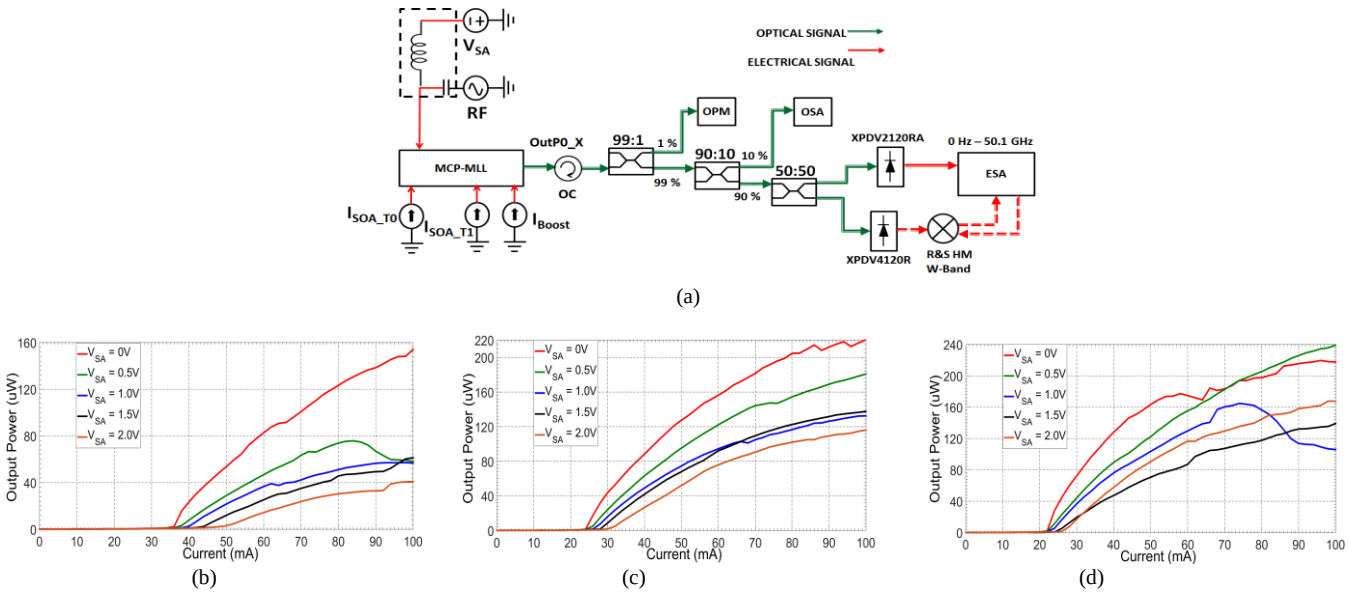

Fig. 2. (a) Sketch of the experimental setup. Four DC sources bias the active sections of the MCPMLL. Three independent current sources I_{SOA_T0}, I_{SOA_T1} and I_{Boost} to forward–bias the outer SOAs, the inner SOAs and the boost are used. One voltage supply for reverse-biasing of the SAs via 67 GHz bias tee which is connected to 40 GHz RF GSG probe is used. Fiber-coupled average optical laser output power at the output waveguide OutP0_0 versus I_{SOA_T1} as I_{Boost} = open, V_{SA} is swept from 0 to -2V in 0.5 V steps and I_{SOA_T0} is set to (b) 10 mA, (c) 20 mA and (d) 30 mA.

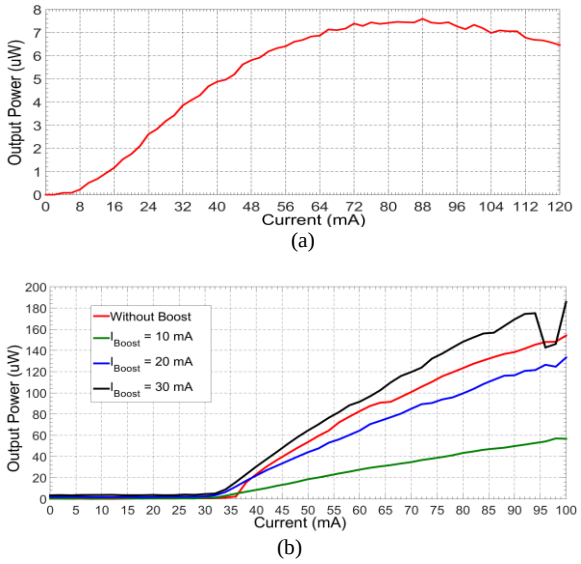

Fig. 3. LI characteristic curve of the boost when (a) I_{SOA_T0}, I_{SOA_T1} and V_{SA} are kept off, the saturation condtion is reached I_{boost} ~ 88 mA and the dP/dI slope is about 0.0655 µW/mA. (b) Optical output power at output port OutP0_1 as I_{SOA_T0} = 10 mA, I_{SOA_T1} is swept from 0 to 100 mA , V_{SA} = 0 V and I_{Boost} is set to 10 mA, 20 mA and 30 mA.

V. Passive Mode-Locking Operation Regime

The MCPMLL is characterized in the passive mode-locking operation regime, i.e. without RF signal injection. The passive mode-locking operation regimes of the device at different biasing conditions are recorded and depicted in Fig. 4 and Fig. 5. Depending on each gain current injected into each gain section of the multi-section device and the applied SAs reverse-bias voltage the device generates different RRs and optical spectra. For all cases, I_{SOA_T1} is swept from 20 to 100 mA and V_{SA} from 0 to -2 V in 0.2 V steps. As we can see in Fig. 4 and Fig. 5, the blue dark zone denotes no optical spectrum is generated by the device, i.e. no optical lasing mode is generated, while the light blue zone shows the generation of a single lasing mode only. As is depicted in Fig. 4(a) and (b), for low gain current values at I_{SOA_T1} and increasing the SAs reverse-biasing voltage, no lasing mode is generated when I_{Boost} is ≤ 20 mA. High gain current levels injected into I_{SOA_T1} are needed to get the generation of optical spectrum with a frequency spacing of 25 GHz which correspond to the fundamental RR. When the same bias condition for I_{SOA_T0}, $I_{SOA\_T1,}$ and V_{SA} are kept, but the DC current signal injected into I_{Boost} is doubled, as shown in Fig. 5(a) and (b), and comparing both cases we note then that the optical spectrum mapping change completely, showing the generation of optical spectra with frequency spacing of 25 GHz, 100 GHz, and > 100 GHz. When I_{SOA_T0} is set to 20 mA the 25 GHz optical signal appears more, as shown in Fig. 5(b) eliminating the red zone where two single modes with a frequency spacing greater than 100 GHz are generated. Doubling both the DC current injected into I_{SOA_T0} = 40 mA (Fig. 4(c)) and the current injected into I_{Boost} = 20 mA (Fig. 4(d)), the orange zone (100 GHz) dominates in both cases, thus multiple colliding conditions have a strong effect under these bias conditions generating the fourth harmonic of the fundamental RR. The generation of an optical signal with a frequency spacing >100 GHz in Fig. 5(c), compared with Fig. 5 (a) is reduced by the increase of $I_{SOA\_T0.}$ The DC current signal injected into the boost has an influence over the performance of the MCPMLL structure. The strong influence of the boost over the performance of the whole structure is not deeply studied in this work. For evaluating the spectral performance on the wavelength domain the optical spectra generated by the device under different bias conditions are

depicted in Fig. 6. Different optical spectra generated by the device are shown in Fig. 6(a) (Single-mode lasing), Fig. 6(b) (25 GHz), Fig. 6(c) (100 GHz) and Fig. 6(d) (>100 GHz). For all cases, the side mode suppression ratio (SMSR) is greater than 25 dB. The multi-section semiconductor laser generates lasing optical modes around 1576 nm. When the optical spacing is greater than 0.8 nm (100 GHz) there is a mode-hopping of the lasing modes generating a dual lasing mode with frequency spacing in the order of THz, i.e. an optical spacing of 5.8794 nm which corresponds to 1.1372 THz is generated, as shown in Fig. 6(d). Regarding the optical frequency comb shown in Fig. 6(b), twenty comb lines are observed where the mode spacing between each optical mode is approximately 0.2 nm, equivalent to 25 GHz in frequency. An inset on the left side of the optical spectrum shows the modal spacing between three optical modes

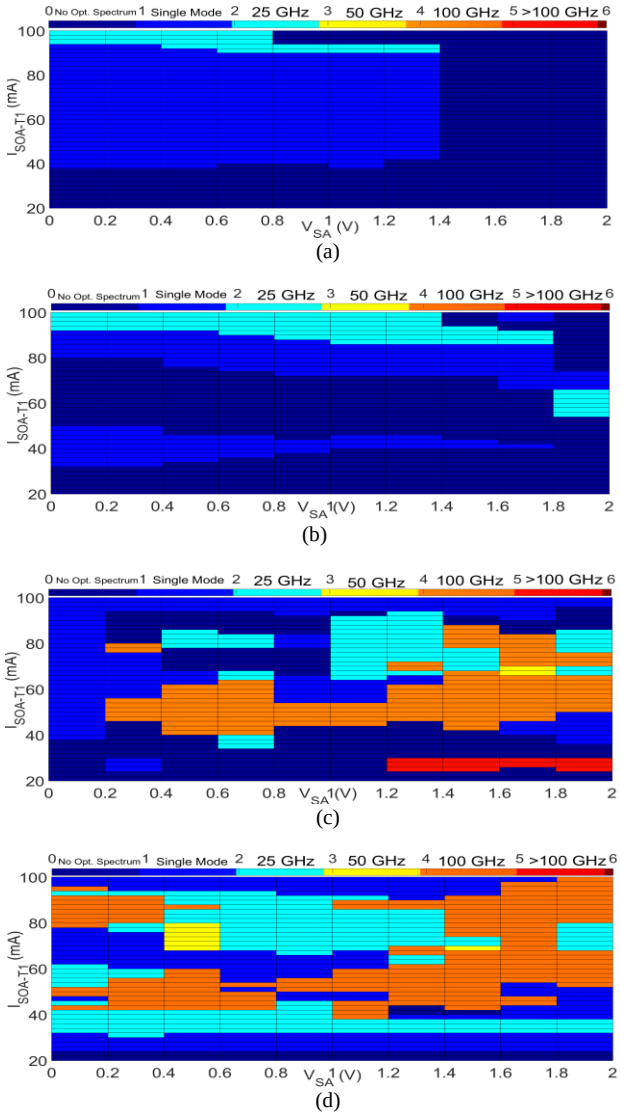

Fig. 4. Optical spectrum mapping of the device measured at output port OutP0_1 at different values of (a) I_{SOA_T0} = 10 mA , (b) I_{SOA_T0} = 20 mA, (c) and (d) I_{SOA_T0} = 40 mA. I_{Boost} is set to 10 mA from (a) to (c) and 20 mA for (d). For all cases I_{SOA_T1} is swept from 20 to 100 mA in 2 mA steps and V_{SA} = 0 to -2 Vin 0.2 V steps.

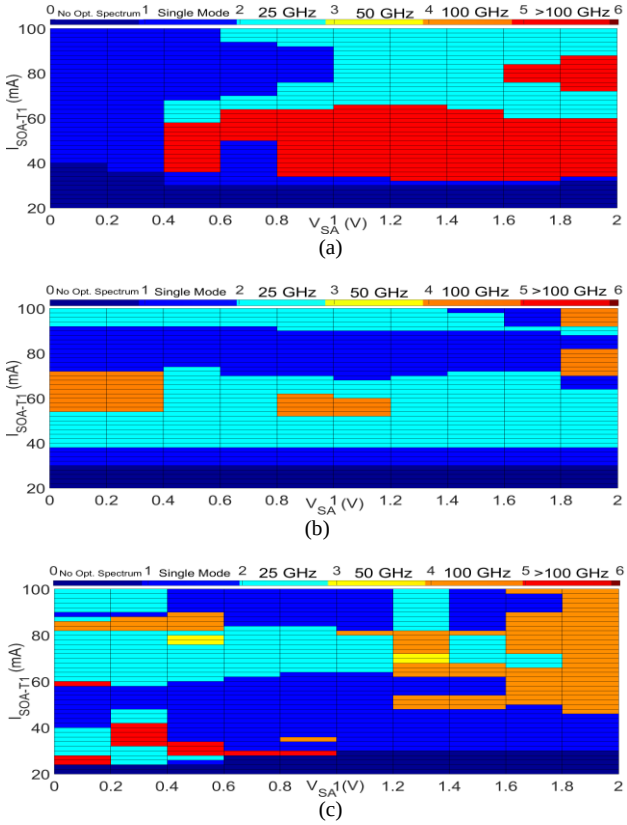

Fig. 5. Optical spectrum mapping of the device measured at output port OutP0_1 at different values of (a) I_{SOA_T0} = 10 mA, (b) I_{SOA_T0} = 20 mA, and (c) I_{SOA_T0} = 50 mA , For all cases I_{Boost} is set to 20 mA, I_{SOA_T1} is swept from 20 to 100 mA in 2 mA steps and V_{SA} = 0 to -2 V in 0.2 V steps.

As we can see in Fig 6(c), the optical spectrum shows seven comb lines and the modal spacing between each lasing mode is around 0.8 nm, which is equivalent to 100 GHz in frequency, the fourth harmonic of the fundamental frequency. The seven lasing modes constitute an optical frequency comb which exhibits a suppression ratio of around 25 dB with respect to the level of the suppressed modes that are associated with the fundamental cavity round-trip frequency of 25 GHz. Only, three lasing modes in every four lasing modes are suppressed, and thus, only one mode in every four lasing modes is excited.

VI. 100 GHz Operation Regime

The fabricated device generates an optical spectrum with an optical spacing of 0.8 nm which correspond to ~100 GHz, four times the fundamental RR (~25 GHz). The measured optical spectrum, depicted in Fig. 7(a), is generated under the passive operation regime. The bias conditions used for obtain this result are the following: I_{SOA_T0} = 30 mA, I_{SOA_T1} = 50 mA, I_{Boost} = 20 mA and V_{SA} = -1.6V. The generated optical spectrum is strongly symmetric with respect to the central lasing mode which lases around 1576 nm. For the RF spectra analysis, the electrical spectrum has been measured and recorded as shown in Fig. 7(b). In fig. 7(b), we can observe the electrical beat-tone generated by the device at 100 GHz in passive operation regime with an electrical linewidth (ELW) of ~400 kHz @-3dB, red solid line. This latter value is less than

the ELW in [22] improving the performance of the device. In order to verify if electrical tones of 50 and 25 GHz are generated at the same time, the electrical spectrum at this frequency range is measured. The result is that no RF electrical tones are observed. To measure the stability of the generated electrical signal, the max-hold operation is carried out thus, the 100 GHz electrical tone has a drift of ±2.5 MHz over 10 min, as shown in Fig. 7(c). The hybrid mode-locking operation regime using electrical injection is achieved when the RF signal injected into the SAs is equal to the frequency spacing of the optical spectrum generated by the laser i.e. if laser generates an optical spectrum with a frequency spacing of 100 GHz, 100 GHz RF signal must be injected into the SAs. Such an RF signal generator with a very low ELW (< 10Hz) and phase noise in order to improve the quality of the generated electrical beating signal is not easy to find.

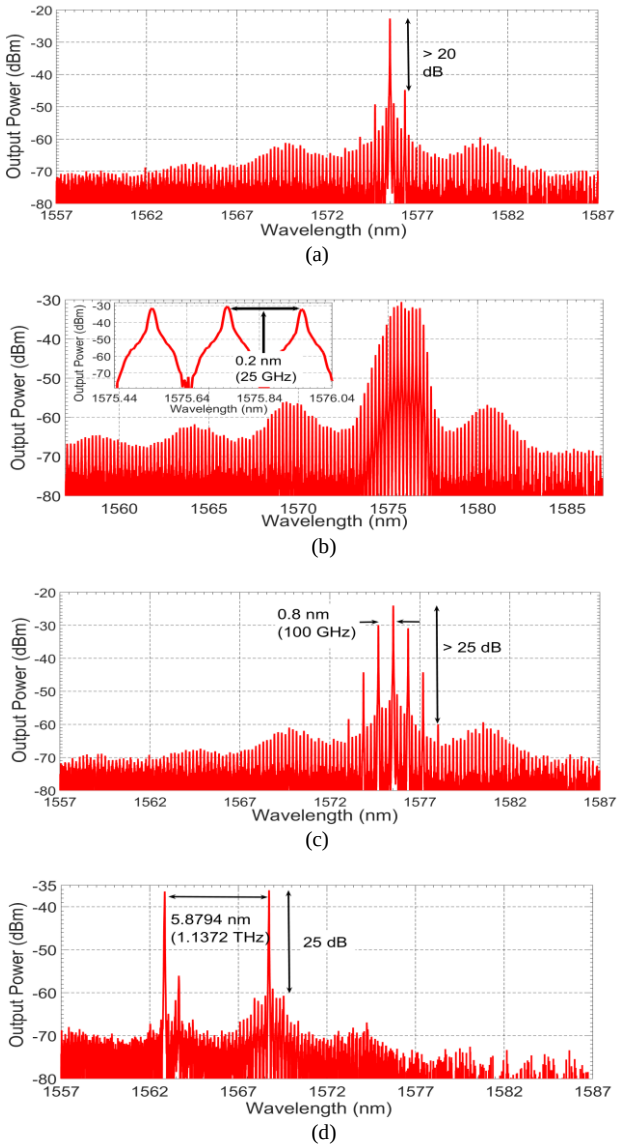

Fig. 6. Optical spectrum of the multi-section semiconductor laser at different bias conditions. (a) single mode lasing. Optical freqeucny comb with a modal spacing of (b) 0.2 nm (25 GHz) and (c) 0.8 nm (100 GHz), (d) Dual lasing mode with optical spacing of 5.8794 nm (1.1372 THz)

In this work, we want to show that using a subharmonic RF signal to lock the optical modes to get hybrid mode-locking operation regime can be achieved. The subharmonic RF signals used for this experiment are the fundamental cavity round-trip frequency and twice the fundamental cavity round-trip frequency i.e. the RF signal frequency should be around 25 and 50 GHz. The RF signal is injected into the SAs via GSG RF probe. The synchronization of the pulses generated by the device with the RF generator connected to the bias tee (Fig. 2(a)) allows us to strongly decrease the phase noise of the electrical beat-tone. To get the first hybrid operation regime, an RF signal of 49.9389 GHz with a power level of 25 dBm is injected. The electrical beat-tone generated by the device in the hybrid mode-locking operation regime is shown in Fig. 7(b) blue solid line. The measured RF signal peak is -48 dBm. For the passive and hybrid operation regimes an RBW = 2 kHz, VBW = 30 Hz and a span = 20 MHz and a central frequency at 49.9389 GHz is used. Under different bias conditions in the passive mode-locking operation regime, the ELW of the beat-tone goes down from 400 to 150 kHz while the peak RF power increases from -70 to -60 dBm. In fact, injecting an RF signal the RF power increases up to -50 dBm and the ELW of the beat-tone is decreased up to the Hz range which is only limited by the quality of the RF generator signal

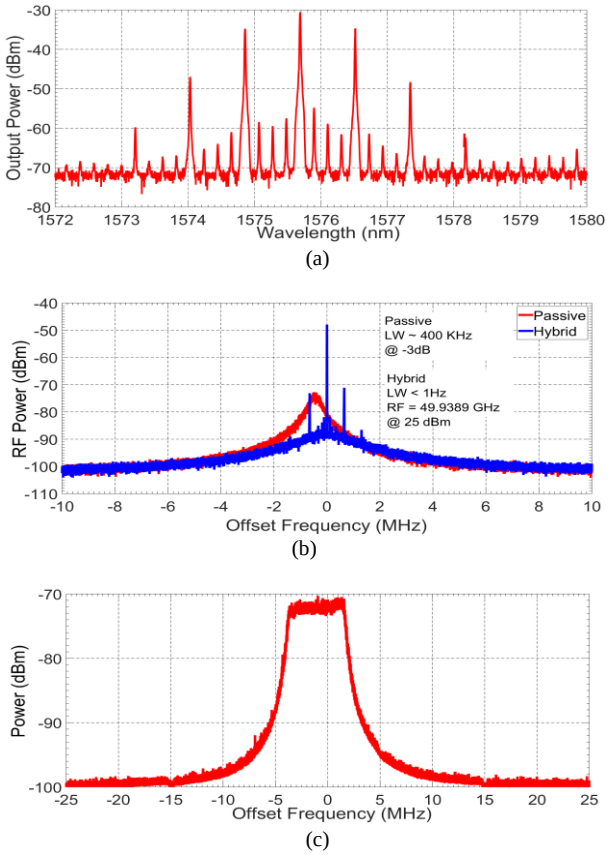

Fig. 7. . Optical and electrical spectrum of the MCPMLL. (a) Optical spectrum with lasing modes separated each 0.8 nm (100 GHz) (b) RF electrical tone in passive (red) and hybrid (blue) operation regimes, the achieved electrical linewidths are ~400 kHz and less than 1 Hz, respectively. (c) Maxhold of the electrical beat-tone over 10 min.

The measured ELW is <1 Hz which is related to the electrical ELW of the RF generator used during this experiment. In fact, an RF signal greater than 20 dBm ought to be injected into the SAs in order to reach almost the maximum noise pedestal suppression. We also tested the device injecting a 25 GHz RF signal to lock and synchronize the pulses generated by the laser to the RF generator but unfortunately, an RF power greater than 25 dBm must be injected to stabilize the electrical beating generated by the laser and thereby reducing the phase noise. In order to know how much RF power must be injected to reduce the phase noise of the electrical beating signal using a lower harmonic of the 100 GHz microwave signal, we have measured the noise pedestal as a function of the RF driving power, as well as the RF output power as a function of the RF input power.In Fig. 8(a), we can see the locking of the electrical beat-tone in passive operation regime via RF driving power in order to get the hybrid operation regime. The RF input power driven by the generator goes from 0 to 25 dBm in 5 dBm steps. As the RF input power increases the RF output power increases up to ~ -47 dBm. In fact, the SMSR increases as the noise pedestal decrease. The higher the RF input power the lower the noise pedestal The effect of decreasing the noise pedestal is due to the increase of modulation depth of the SAs. The performance of the RF output peak signal and the noise pedestal is shown in Fig. 8 (b). The optical spectra generated by the multi-section semiconductor laser as the RF input power is swept from 0 to 25 dBm at ~50 GHz are shown in Fig. 9(a) (RF = 0) dBm, Fig. 9(b) (RF = 5 dBm), Fig. 9(c) (RF = 10 dBm), Fig. 9(d) (RF = 15 dBm), Fig. 9(e) (RF = 20 dBm) and Fig. 9(f) (RF = 25 dBm). From Fig. 9(c) to Fig. 9(f), the optical spectrum exhibits that the optical lasing modes with a frequency spacing linked to the RF generator signal are risen up and is partly attributed to the efficient microwave coupling into the device [25].

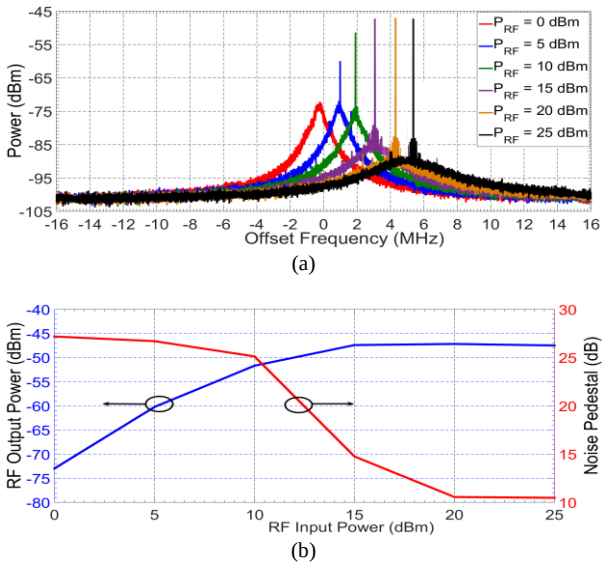

Fig. 8. (a) Electrical spectrum of the hybrid mode-locking regime at different RF input power. Higher RF input power higher SMSR. The locking range was found to be about 6 MHz. (b) Analysis of the RF output power and Noise pedestal versus RF input power injected into the SAs.

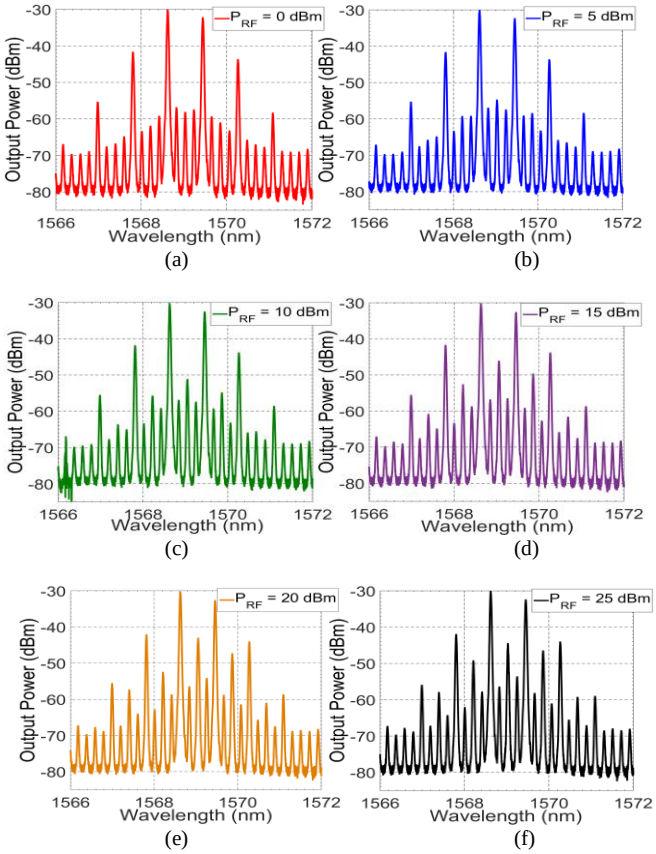

Fig. 9. Evolution of the optical spectrum generated by the structure at different values of RF input power. The RF input power is swept from 0 to 25 dBm in 5 dBm steps. (a) P_{RF} = 0 dBm, (b) P_{RF} = 5 dBm, (c) P_{RF} = 10 dBm, (d) P_{RF} = 15 dBm, (e) P_{RF} = 20 dBm and (f) P_{RF} = 25 dBm

VII. Conclusions

We have successfully presented an InP mode-locked semiconductor laser for 100-GHz optical frequency comb generation. The laser cavity features multiple segments in a symmetric arrangement in which short SOAs separate the overall 1.66-mm-long resonator into four shorter divisions in equal length to achieve fourth harmonic generation. The on-chip multimode interference reflectors have shown the potential to replace the cleaved facets.

References

[1] T. Nagatsuma, and G. Carpintero, "Recent Progress and Future Prospect of Photonics-EnabledTerahertz Communications Research," in *IEICE Trans Electron*," vol E98, no. 12, 1060-1070, 2015

[2] E. Avrutin, J. Marsh, and E. Portnoi, "Monolithic and multi-gigahertz mode-locked semiconductor lasers: constructions, experiments, models and applications," *IEEE Proceedings-Optoelectronics*, vol. 147, no. 4 251–278 (2000).

[3] R. G. Broeke, J. Cao, C. Ji, S.-W. Seo, Y. Du, N. K. Fontaine, J.-H. Baek, J. Yan, F. M. Soares, F. Olsson, S. Lourdudoss, A.-V. H. Pham, M. Shearn, A. Scherer, and S. J. B. Yoo, "Optical-CDMA in InP," *IEEE J. Sel. Top. Quant. Electron*. 13, 1497–1507, 2007

[4] P. J. Delfyett, A. Ardey, S. P. Bhooplapur, and E. Sarailou, "InP-based device technologies for signal processing using ultrafast frequency combs," *IEEE Optics Letter*. 42, 2318 - 2321, 2017.

[5] Guzmán R. Gordon, C., Orbe. L, Carpintero G. "1 GHz InP On-Chip Monolithic extended Cavity Colliding-Pulse Mode-Locked Laser," *IEEE Opt. Lett*. Vol 42, no 12, 2318– 2321, 2017.

[6] S. Liu, X. Wu, D. Jung, J. C. Norman, M. Kennedy, H. K. Tsang, A. C. Gossard, and J. E. Bowers, "High-channel-count 20 GHz passively mode-locked quantum dot laser directly grown on si with 4.1 tbit/s transmission capacity," *Optica*, vol. 6, no. 2, pp. 128–134, 2019

[7] A. S. Raja, A. S. Voloshin, H. Guo, S. E. Agafonova, J. Liu, A. S. Gorodnitskiy, M. Karpov, N. G. Pavlov, E. Lucas, R. R. Galiev, et al., "Electrically pumped photonic integrated soliton microcomb," *Nature Communications*, vol. 10, no. 1, p. 680, 2019

[8] J. H. Marsh and L. Hou, "Mode-locked laser diodes and their monolithic integration," *IEEE J. Sel. Top. Quantum Electronics*, vol. 23, no. 6, 1-11.

[9] Y. K. Chen, M. C. Wu, T. Tanbun-Ek, R. A. Logan, and M. A. Chin, "Subpicosecond monolithic colliding-pulse mode-locked multiple quantum well lasers," *Appl. Phys. Lett.,* vol 58,no 12, 1253–1255, 1991.

[10] C. Gordon, R. Guzman, V. Corral, X. Lijtens, and G. Carpintero, "On-chip colliding pulse mode-locked laser diode (OCCP-MLLD) using multimode interference reflectors," *Journal of Lightwave Technology*, vol. 34, no. 20, pp. 4722–4728, 2016

[11] A. Avrutin, J. H. Marsh, J. M. Arnold, T. F. Krauss, H. Pottinger, and R. M. D. la Rue, "Analysis of harmonic (sub) THz passive mode-locking in monolithic compound cavity Fabry-Perot and ring laser diodes," *IEEE Proc. – Optoelectronics*, vol. 146, no. 1, 55–61, 1999.

[12] S. Arahira, S. Oshiba, Y. Matsui, T. Kunii, and Y. Ogawa, "Terahertz-rate optical pulse generation from a passively mode-locked semiconductor laser diode," *Opt. Lett.*, vol. 19, no. 11, 834–836, 1994.

[13] L. Hou, M. Haji, R. Dylewicz, P. Stolarz, B. Qiu, E. Avrutin, and A. Bryce, "160 GHz harmonic mode-locked AlGaInAs 1.55μm strained quantum-well compound-cavity laser," *Opt. Lett.* 35, 3991-3993, 2010

[14] Y. Katagiri and A. Takada, "A harmonic colliding-pulse mode-locked semiconductor laser for stable subterahertz pulse generation," *IEEE Photonics Technol. Lett.*, vol. 9, no. 11, 1442–1444, 1997.

[15] J. F. Martins-Filho, E. A. Avrutin, C. N. Ironside, and J. S. Roberts, "Monolithic multiple colliding pulse mode-locked quantum-well lasers, experiment and theory," *IEEE J. Sel. Top. Quantum Electronics*, vol.1, no.2, 539–551, 1995.

[16] L. Hou, M. Haji, and J. H. Marsh, "240 GHz pedestal-free colliding-pulse mode-locked laser with a wide operation range," *Laser Phys. Lett.* , vol. 11, no. 11, pp. 115804, 2014

[17] M. Lo, R. Guzmán, and G. Carpintero, "Femtosecond pulse and terahertz two-tone generation from facet-free multi-segment laser diode in InP-based generic foundry platform," *Opt. Express* vol. 26, no 14, 18386-18398 2018.

[18] E. Kleijn, M. K. Smit, and X. J. Leijtens, "Multimode interference reflectors: a new class of components for photonic integrated circuits," *J. Light. Technol.*, vol. 31, no. 18, 3055–3063, 2013.

[19] S. Stopinski, M. Malinowski, R. Piramidowicz, C. Kazmierski, M. K. Smit, and X. J. Leijtens, "Photonic integrated multichannel wdm modulators for data read-out units," *J. Light. Technol*., vol. 32, no.23, 3879–3887, 2014.

[20] M. P. E. Morrissey, N. Kelly, M. Dernaika, L. Caro, H. Yang, and F. H. Peters, "Coupled cavity single-mode laser based on regrowth-free integrated MMI reflectors," *IEEE Photonics Technol. Lett.*, vol. 28, no.12, 1313–1316, 2016.

[21] M.-C. Lo, R. Guzmán, C. Gordón, and G. Carpintero, "Mode-locked laser with pulse interleavers in a monolithic photonic integrated circuit for millimeter wave and terahertz carrier generation," *Opt. Lett.*, vol. 42, no. 8, 1532–1535, 2017.

[22] C. Gordon, R. Guzman, V. Corral, M. C. Lo, and G. Carpintero, "On-chip multiple colliding pulse mode-locked semiconductor laser," *Journal of Lightwave Technology*, vol. 34, no. 20, pp. 4722–4728, 2016

[23] R. Guzmán, G. Carpintero, C. Gordon and L. Orbe, "Millimeter-wave signal generation for a wireless transmission system based on on-chip photonic integrated circuit structures," *Opt. Lett.*, vol. 41, no. 20, 4843–4846, 2016

[24] Smart Photonics. [Online]. Available at https://smartphotonics.nl/ , 2018.

[25] T. Hoshida, L. Hai-Feng, M. Tsuchiya, Y. Ogawa and T. kamiya, "Subharmonic Hybrid Mode-Locking of a Monolithic Semiconductor Laser," *IEEE J. Sel. Top. Quantum Electronics*, vol.2, no.3, 514–522, 1996.

Robinson C. Guzmán Martínez was born in Barranquilla, Atlántico, Colombia. He received the Electronics Engineering degree and the Industrial Electronic Specialist degree from the Universidad del Norte de Barranquilla, Colombia, in 2003 and 2005, respectively, the Informatics and Telematics Specialist degree from the Universidad del Area Andina in 2006, and the master's degree in advanced electronics systems and the Ph.D. degree in electrical engineering, electronics and automation from the Carlos III University of Madrid (UC3M) in 2011 and 2016, respectively. He has been with the Optoelectronics and Laser Technology Group (GOTL), UC3M, in 2009. Since 2009, his research activities and interest has been focused on microwave photonics (MWP), photonic integrated circuits (PICs) design, millimeter-wave, and terahertz signal generation based on photonic integrated circuits for high-data rate wireless communication, low-frequency microwave signals generation based on photonic integrated circuits, and wireless link transmission system design

Jessica Cesar Cuello was born in Artemisa, Cuba. She received the degree in telecommunication and electronics engineering from the Technological University of Havana in 2011, and the M Sc. degree in engineering of electronic systems and applications from the University Carlos III de Madrid (UC3M) in 2018, where she is currently pursuing the Ph.D. degree. From 2011 to 2017, she worked with the Telecommunications sector, more specifically in the area of private telephone centers installing and programming them. Her research interests include the field of microwave photonics and the design of photonics integrated circuits.

Alberto Zarzuelo was born in Spain. He received the bachelor's degree in industrial electronics and automation engineering and the master's degree in electronic systems engineering from the Universidad Carlos III de Madrid (UC3M) in 2016 and 2017, respectively. He is currently pursuing the Industrial Ph.D. degree with SENER aerospace and UC3M developing low phase noise sources for satellite flexible payloads. During that time, he was involved in a project called DIFRAGEOS, where he was worked on fiber gratings. His research interests include photonic integrated circuits (PICs) for microwave, millimeter, and THz wave generation techniques.

Mu-Chie Lo received the B.Eng. degree from the National Taiwan University, the M.Sc. degree from the Technische Universität Berlin and the Scuola Superiore Sant'Anna, and the Ph.D. degree from the Universidad Carlos III de Madrid. His research interests include the design, realization, and demonstration of high-speed photonic integrated circuits for optical communication systems. Dr. Lo is currently Marie Curie Fellow at University College London.

Muhsin Alí received the B.Sc. degree in telecommunication engineering from FAST-NUCES, Pakistan, in 2011 and the M.Sc. degree in electrical engineering from NUST, Pakistan, in 2013. He is currently pursuing the Ph.D. degree with the Department of Electronics Technology, Universidad Carlos III de Madrid (UC3M), Spain, funded by EU Horizon 2020 ITN titled FiWiN5G. His professional experience includes working as an RF Engineer in Saudi Arabia for deployment of Huawei's 4G/LTE network. His research activities antenna-integrated photonic millimetre-wave and terahertz sources, Schottky diode-based detectors, wireless communication, and photonic phased array antenna for beamforming

Guillermo Carpintero del Barrio received the Engineering degree from the Universidad Politécnica de Madrid and the Ph.D. degree from UC3M. He is currently a Full Professor with the Electronics Technology Department, Carlos III University of Madrid (UC3M). He has been a Visiting Researcher with the Center for Advanced Photonics and Electronics (CAPE), University of Cambridge, and a Visiting Professor with University College London and Osaka University. He was awarded the Heather Williamson Young Investigator Award in 2000 from the International Society for Optics and Photonics (SPIE), the Award of Excellence Social Council of UC3M in 2009, and the Award for Best European R&D Project in Cooperation MadrI+D Foundation in 2011. He is on the Editorial Board of the *IET Optoelectronics Journal*.